

# NANOENGINEERED INDUCTIVELY COUPLED CARBON NANOTUBE WIRELESS STRAIN SENSOR

K. J. Loh, J. P. Lynch, and N.A. Kotov

*Department of Civil & Environmental Engineering, University of Michigan, Ann Arbor, MI 48109 USA*  
[kenloh@umich.edu](mailto:kenloh@umich.edu), [jerlynch@umich.edu](mailto:jerlynch@umich.edu), [kotov@umich.edu](mailto:kotov@umich.edu)

## Abstract

Since the discovery of carbon nanotubes by Iijima in 1991, researchers have utilized carbon nanotubes for a wide array of applications including nanoelectronics, sensors, and inductively coupled antennas. While current and novel strain transducers can measure strain adequately, their large form factor and cabled data acquisition systems render their use in harsh environments difficult. It has been demonstrated from early experimental studies that conformable carbon nanotube/polyelectrolyte thin films exhibit linear changes in resistivity with applied strain. By patterning these films into coil antenna patterns, a passive inductively coupled wireless strain sensor is fabricated and presented. Antenna resonant frequency and bandwidth is characterized, and the overall response represents that of a series RLC resonant circuit. It is shown that the wireless nanotube strain sensor shows corresponding changes in bandwidth to applied strain. To optimize the performance of the carbon nanotube composite antenna, electrochemical impedance spectroscopy is employed to fully characterize the bulk electrical properties of the carbon nanotube/polyelectrolyte thin films.

## Introduction

In recent years, carbon nanotubes have been utilized for a wide range of applications including high-strength structural composites (Andrews *et al.*, 1999), nanoelectronics (Tsukagoshi *et al.*, 2002), various types of sensors (Kong *et al.*, 2000 and Wood *et al.*, 2000), inductively coupled antennas (Ong *et al.*, 2002), among many others (Baughman *et al.*, 2002). Since the discovery of carbon nanotubes (Iijima, 1991), researchers have sought to take advantage of their superior mechanical (Salvetat *et al.*, 1999) and electrical properties (Baughman *et al.*, 2002) for the aforementioned applications. For example, the Young's modulus and ultimate tensile strength of individual single-walled carbon nanotubes (SWNTs) have been estimated to be approximately  $E \approx 1,054$  GPa and  $\sigma_f \approx 75$  GPa, respectively, rendering them candidates for use in ultra-strength composites (Meyyappan, 2005). Similarly, the high electrical conductivity of carbon nanotubes owe to their one-dimensional structure offering near-ballistic transport-type electronic behavior (Baughman *et al.*, 2002).

Among the wide array of carbon nanotube applications, researchers in the health monitoring community have sought to utilize the piezoresistive nature of carbon nanotubes and their composites for sensing transducers (Dai, 2002). Particularly, strain sensing has been important for measuring component-level strain in the laboratory and in the field for structural damage diagnosis. While current metal-foil strain gauges, semiconducting strain sensors, and fibre optic Bragg gratings achieve high sensitivities, they typically suffer from high manufacturing costs and large form factors, thus limiting their adoption in certain environmental conditions. As opposed to a "top-down" sensor design paradigm adopted in micro-electromechanical systems (MEMS), researchers can undertake a "bottom-up" approach by utilizing nanotechnology to design a new class of strain sensors at the molecular length-scale.

Pioneering strain sensing experimental studies performed by Tomblor *et al.* (2000), Peng *et al.* (2001), and Minot *et al.* (2003) have shown that individual carbon nanotubes suspended over patterned silicon substrate trenches under atomic force microscopy (AFM) tip manipulation exhibit extreme changes in conductance. Instead of manipulating individual nanotubes in a controlled environment, Dharap *et al.* (2004) and Li *et al.* (2004) have fabricated nanotube thin films known as "buckypaper" and have identified linear changes in voltage as the "buckypaper" is strained under low tensile-compressive cyclic

loading ( $\epsilon \leq \pm 400 \mu\text{m}/\text{m}$ ). A recent experimental study conducted by Loh *et al.* (2006) varies the fabrication parameters of carbon nanotube composite films to optimize the thin films' strain sensor gauge factor and capacitance. Equivalent parallel-RC circuit models fit experimental data and characterizes the electrical-mechanical behavior of the thin film during tensile-compressive cyclic loading ( $\epsilon \leq \pm 0.005 \text{ m}/\text{m}$ ).

In recent years, wireless sensors have been proposed for structural monitoring (Lynch and Loh, 2005). While the majority of these wireless sensors are an integration of wireless modems and microcontrollers with sensing transducers, a small class of wireless sensors that require no power have recently emerged. Such wireless sensors are powered and read using inductive coupling (Mita and Takhira, 2004). Inductive coil antennas coupled with strain transducers can modulate strain measurements onto a carrier frequency and transfer sensor outputs wirelessly to a remote receiver. In this study, carbon nanotube thin films will be patterned into coil antennas to detect strain. By patterning carbon nanotube thin films, an inductively coupled antenna can be fabricated from an RC-circuit-type thin film; strain can be detected via shifts in the coil antenna's characteristic frequency or changes in its bandwidth due to changes of its  $R$  and  $C$  values. One example of patterning nanotube films has been presented by Ong *et al.* (2002) which utilizes multi-walled carbon nanotubes (MWNT)-silicon dioxide ( $\text{SiO}_2$ ) patterned antennas to monitor carbon dioxide ( $\text{CO}_2$ ), oxygen ( $\text{O}_2$ ) and ammonia ( $\text{NH}_3$ ).

In this paper, an inductively coupled wireless SWNT-polyelectrolyte (PE) thin film strain sensor is presented. Using a layer-by-layer (LBL) self assembly process, SWNT-PE conformable macro-scale thin films are fabricated for strain sensing. SWNT-PE strain sensing properties are optimized for maximum gauge factor by using high concentration SWNT and PE solutions (Loh *et al.*, 2006). First, the characteristic frequency of the antenna is identified using an impedance/gain phase analyzer. SWNT-PE antenna specimens are subjected to cyclic tensile loading to investigate changes in their characteristic frequencies and bandwidths. Finally, optimization of wireless strain sensing is accomplished by conducting electrochemical impedance spectroscopy (EIS) studies on bulk SWNT-PE thin films.

## SWNT-PE Thin Film Fabrication

### *Layer-by-Layer Assembly*

Fabrication of multilayer carbon nanotube-polyelectrolyte composite thin films is accomplished using a layer-by-layer (LBL) self-assembly process (Decher, 1997, Kotov, 2001, and Paloniemi *et al.*, 2006) as shown in Figure 1. In general, the LBL method employs the sequential deposition of oppositely charged species to form multilayer films. Adsorption of each monolayer is based on opposite charge electrostatic and van der Waals force interaction with its previous monolayer (Mamedov *et al.*, 2002, Olek *et al.* 2004, and Rouse and Lillehei, 2003). By depositing a charged species, followed by an oppositely charged one, a uniform composite bilayer can be deposited on the substrate. Multilayer thin films of desired thicknesses can be fabricated by controlling the number of bilayers deposited upon the substrate.

The LBL process begins by first immersing a biaxially oriented polyethylene terephthalate (boPET) thin film substrate in a 1.0% *by wt.* poly(vinyl alcohol) (PVA, Sigma) solution for 5 min to deposit the initial polyelectrolyte monolayer. Upon completion, the substrate is rinsed in 18 MOhm deionized water for 3 min and subsequently dried (compressed air jet) for 15 min. Prior to depositing the second opposite charged monolayer, single-walled carbon nanotubes are dispersed in a solution of 1.0% *by wt.* poly(sodium 4-styrene-sulfonate) (PSS, 1,000,000  $M_w$ , Aldrich) to form 0.50 mg/mL SWNT-PSS solutions. Steric stabilization of nanotube solutions is achieved by treating the SWNT-PSS solution with 180 min of ultrasonication bath (135 W, 42 kHz) followed by 90 min of high-powered tip deep sonication

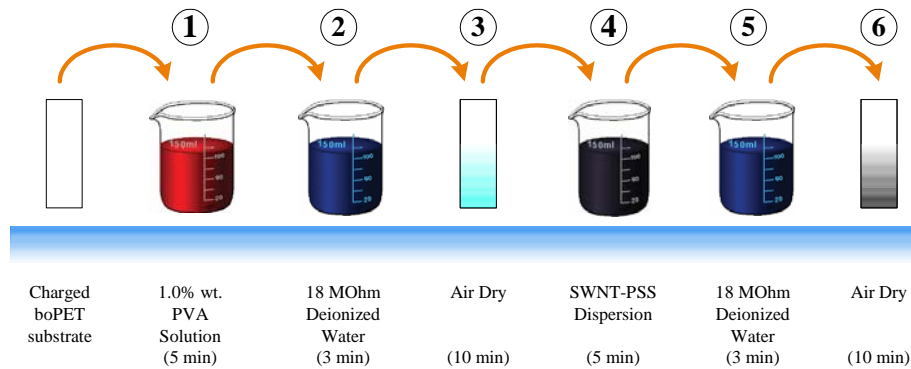


**Figure 1. Illustration of the layer-by-layer self-assembly process to fabricate SWNT-PE thin films (Loh *et al.*, 2006).**

at 30% amplitude (3.175 mm tip, 500 W, 22.0 kHz). Deposition of the second monolayer continues by dipping the dried substrate in the dispersed SWNT-PSS solution for 5 min, followed by rinsing in deionized water for 3 min and 15 min of drying. This process completes the deposition process for one SWNT-PSS/PVA bilayer and is repeated numerous times to fabricate films of desired thicknesses (*e.g.* 50, 100, 200 bilayers).

#### *Optimization for Strain Sensing*

Optimization of SWNT-PSS/PVA thin films for strain sensing is accomplished by fabricating films of high gauge factor ( $GF = (\Delta R/R)/\varepsilon$ , where  $R$  is film resistance and  $\varepsilon$  is applied strain). Earlier studies (Loh *et al.*, 2005 and Loh *et al.*, 2006) have shown that LBL fabrication parameters can be tailored to fabricate films of specific gauge factor ( $GF$ ), resistivity, and capacitance. Gauge factors between 0.01 and 100 have been experimentally characterized for films fabricated with different LBL fabrication parameters, namely SWNT concentration, PSS concentration, and film thickness. Results presented by Loh *et al.* (2006) indicate that films fabricated with 0.50 and 0.80 mg/mL SWNT dispersed in 1.0% PSS *by wt.* exhibit the highest sensitivity to strain (Figure 2). Furthermore, thinner 50-bilayer multilayer films exhibit higher gauge factor than thicker SWNT-PSS/PVA films (100- and 200-bilayers). Although minor nonlinear response is observed during tensile-compressive cyclic loading, the piezoresistivity of the SWNT-PSS/PVA thin films can be adequately described using an equivalent parallel-RC circuit. Equivalent gauge factors for  $R$  and  $C$  can be deduced based on numerical analysis of thin film response (Loh *et al.*, 2006). For this study, 0.50 mg/mL SWNT dispersed in 1.0% PSS (*by wt.*) is employed to fabricate 50-bilayer thin films; a patterned thin film specimen is shown in Figure 3.

### **Inductively Coupled Passive Wireless Carbon Nanotube-Based Antenna**

#### *Inductively Coupled Coil Antenna and Radio Frequency Identification (RFID) Background*

A typical radio frequency identification (RFID) system is comprised of an inductor ( $L$ ), capacitor ( $C$ ), and resistor ( $R$ ) organized in parallel or in series. While the resistor and capacitor chosen for the circuit can tune the resonant frequency and bandwidth of the RFID system, the most important component is the antenna coil (inductor). The antenna coil is used to wirelessly receive power transmitted by the reader as well as resonate information (*e.g.* sensor readings) back to the reader. To transmit power to the passive inductively coupled tags, the reader generates a strong, high frequency electromagnetic (EM) field to cause a voltage drop in the tag antenna coil (Finkenzeller, 1999). Typically, a series or parallel resonant circuit can be formulated depending on the specific application. In a series resonant circuit (Figure 4),

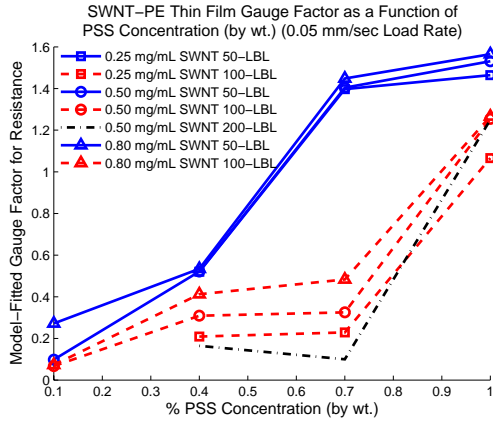


**Figure 2: Gauge factor calculated from tensile-compressive cyclic loading for different SWNT-PSS/PVA thin films as a function of PSS concentration.**



**Figure 3: Patterned SWNT-PSS/PVA thin film inductively coupled wireless coil antenna.**

minimum impedance occurs at the resonant frequency, thus providing maximum current at resonance; on the other hand, a parallel resonant circuit yields maximum impedance and minimum current at resonance (Lee, 1998). Based on the series resistor ( $R$ ), capacitor ( $C$ ), and inductor ( $L$ ), the half power frequency bandwidth ( $B$ ) can be determined by equation (1).

$$B = \frac{R}{2\pi L} \text{ (Hz)} \quad (1)$$

The bandwidth of the resonant circuit can be decreased by reducing the overall film resistance (*i.e.* through chemical cross-linking of films or thermal annealing) and by increasing the inductance by patterning more coils. Similarly, the resonant frequency ( $f_c$ ) for the SWNT-PSS/PVA wireless strain sensor can be tuned by equation (2) (Lee, 1998 and Finkenzeller, 1999).

$$f_c = \frac{1}{2\pi\sqrt{LC}} \text{ (Hz)} \quad (2)$$

### Experimental Setup

Upon completion of the layer-by-layer assembly process, SWNT-PSS/PVA thin films along with their boPET substrate are cut to 15 mm x 25 mm rectangles. A Dremel rotary tool is employed to pattern the coil-antenna by cutting away the film and substrate simultaneously. To ensure dust and film particles do not affect the measurement results, a compressed air jet is employed during the patterning phase to remove foreign particles. The resulting antenna is subsequently affixed to 3.8 cm x 30.5 cm x 1.9 cm PVC (Type I) bars using CN-E epoxy (Tokyo Sokki Kenkyujo) (Figure 3). The specimens are allowed to dry for six hours to ensure perfect bonding before commencing testing.

### Identifying Coil Antenna Properties

In order to identify the resonant frequencies of the patterned SWNT-PSS/PVA thin film coil antennas, a Solartron 1260 Impedance/Gain Phase analyzer is employed. With the capability of generating AC signals between 1 Hz to 32 MHz with a resolution of 0.1 Hz, precise resonant frequency identification can

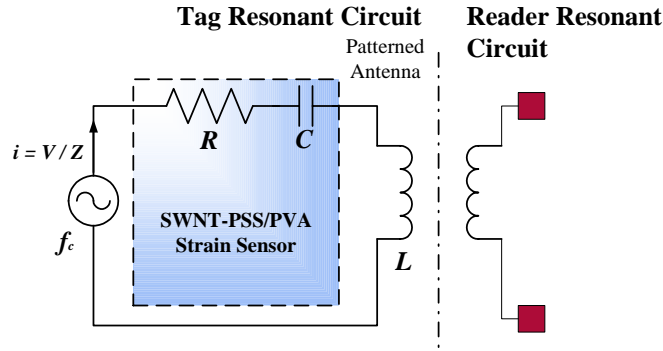


**Figure 4. Series RLC-resonant circuit illustration for typical inductive coil antenna applications.**

be accomplished. Furthermore, to ensure accurate impedance measurements, a four-terminal technique is utilized to prevent errors caused by stray capacitance and impedance of the connection cables. A representative plot of the impedance phase and magnitude of the SWNT-PSS/PVA antenna shown in Figure 3 is presented in Figure 5. For the sample shown, the characteristic frequency has been identified as 14.7 MHz. Other SWNT-PSS/PVA thin film coil antennas exhibit resonant frequencies between 8 and 17 MHz, depending on the number of coils and LBL fabrication parameters.

#### *SWNT-PSS/PVA Coil Antenna Strain Sensor Validation*

Once the resonant frequency has been successfully identified, characterization of changes in resonant frequency and bandwidth under applied strain are investigated by applying a tensile cyclic load pattern to various SWNT-PSS/PVA coil antenna samples. An MTS-810 load frame is employed to apply a one-cycle tensile load pattern to 0.8% strain ( $\epsilon = 0.008 \text{ m/m}$ ), and the coil antenna impedance frequency response is recorded at every 0.2% strain increment. The load rate of the MTS-810 load frame is set at 0.03 mm/sec to prevent damage occurring to the specimens. The antenna's impedance response is automatically recorded from the Solartron 1260 Impedance/Gain Phase analyzer via a GPID interface connected to a computer. A representative plot of the antenna bandwidth calculated at  $Z_{mag} = 8,700 \text{ Ohms}$  for the different applied strain states is shown in Figure 6. From Figure 6, it is obvious that the SWNT-PSS/PVA antenna bandwidth changes in tandem with applied strain (as expected due to the change in  $R$  influencing equation 1). Over the range of  $\epsilon \leq 0.8\%$ , the bandwidth increases by approximately 100 kHz. This large increase in bandwidth shows promise for radio frequency identification applications to correlate changes in strain to changes in an antenna bandwidth.

### **Electrochemical Impedance Spectroscopy**

Although the as-fabricated SWNT-PSS/PVA coil antennas show promise for wireless strain sensing, optimization of the strain sensing properties of the antennas can be accomplished by employing electrochemical impedance spectroscopy (EIS) to characterize SWNT-PSS/PVA thin films and subsequent antenna properties (*i.e.* resonant frequency and bandwidth). The primary advantage for utilizing impedance spectroscopy is that it is a powerful and methodical analytical tool capable of characterizing the electronic properties of materials including SWNT-PE thin films. In addition, experimentally obtained EIS data can be mathematically fitted to an empirical equivalent circuit to model its behavior under a variety of external stimuli. In this study, the external stimulus of interest is strain and how it affects the frequency response behavior of SWNT-PSS/PVA thin film coil antennas. In general, impedance spectroscopy experiments are conducted by applying an electrical stimulus of known voltage or current to a time-invariant sample of interest and measuring the resulting response (current or voltage).

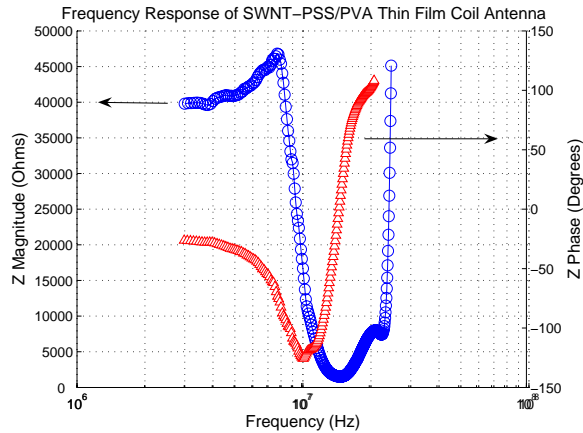


**Figure 5: Frequency response of impedance magnitude and phase for SWNT-PSS/PVA inductively coupled coil antenna.**

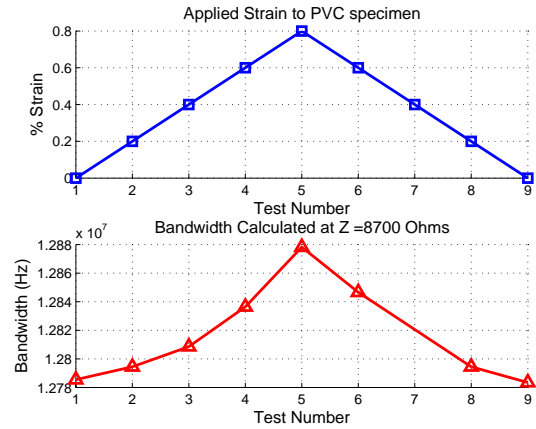


**Figure 6: (Top) applied tensile cyclic load pattern; (bottom) bandwidth change of the coil antenna corresponding to the applied strain.**

Using analog circuit models or the fast Fourier Transform (FFT), one can measure impedance phase shifts and amplitudes of the system's response to the applied single-frequency voltage or current. A real-imaginary plot of the measured impedance ( $Z$ ) provide a graphical depiction of the thin-film resistance (correlated to  $Re(Z)$ ) and capacitance (correlated to  $Im(Z)$ ) over a sweep of electrical signal frequencies (Barsoukov and Macdonald, 2005).

To fully understand the frequency response behavior of SWNT-PSS/PVA thin films under strain, EIS is conducted on a 10 mm x 25 mm rectangular SWNT-PSS/PVA thin film fabricated with the same LBL process and epoxy mounted to a Type I PVC bar. Using the Solartron 1260 Impedance/Gain Phase analyzer, a four-terminal experimental setup is utilized to measure the impedance magnitude and phase from 15 – 250 kHz. First, to verify that the system is time invariant, five EIS measurements are taken 10 min apart on the unloaded specimen. The resulting Nyquist plot shown in Figure 7 suggests negligible change in impedance over time. Changes in position of the Nyquist plots for each of the five measurements cannot be correlated to the time of measurement. Consequently, Figure 7 can be used to describe the noise floor of the EIS data on this particular SWNT-PSS/PVA thin film.

Upon verification that the specimen is indeed time invariant, thus making it suitable for EIS characterization, the affixed film and PVC specimen is loaded monotonically to 1.0% strain ( $\epsilon = 0.010$ ). Impedance spectroscopy is conducted at every 0.25% strain increment while the specimen is held at that strain state; the results are presented in Figure 8. Immediately, it can be seen that there is a near-linear leftward shift as strain is increased from 0% to 1.0%. The constant shift in the arc suggests that the resistance of the thin film is changing in tandem with applied strain. At the peak of the arc, the semi-circles appear to be flattening with increasing strain, thereby suggesting some inherent gauge factor for the thin film capacitance.

## Conclusions

This paper presents a prototype layer-by-layer self-assembled carbon nanotube wireless passive thin film strain sensor (Figure 3). By patterning coil antenna patterns on SWNT-PSS/PVA thin films, preliminary results have successfully identified the resonant frequency of various different antennas, all exhibiting behavior expected for a series RLC resonant circuit (Figure 4 and 5). Upon affixing the SWNT-PSS/PVA

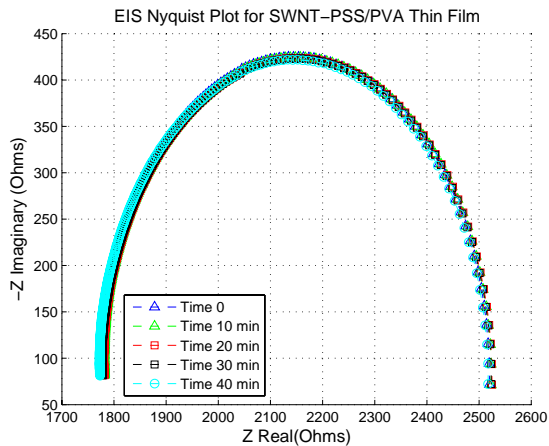


**Figure 7: Nyquist plot for SWNT-PSS/PVA thin film as a function of time to determine time-invariant properties.**

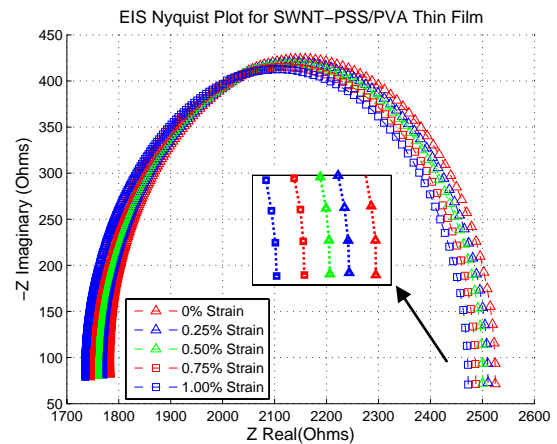


**Figure 8: Nyquist plot for strained SWNT-PSS/PVA thin films; inset shows magnified Nyquist plot for 15 – 20 kHz.**

thin film onto a PVC specimen and subjecting them to cyclic tensile strain, the bandwidth of the coil antenna changes in tandem with changes in strain (Figure 6). However, to optimize the nanotube-based coil antenna for strain sensing, electrochemical impedance spectroscopy is employed to investigate the thin films' frequency domain characteristics under applied monotonic strain. Results from the presented Nyquist plots indicate the system is time-invariant, making it suitable for EIS characterization (Figure 7). Furthermore, a linear shift in the semi-circle is observed, thus suggesting linear changes in film resistivity with strain (Figure 8). Although a minor change in arc is seen from the Nyquist plots, the overall capacitive strain sensitivity is low. In order to achieve resonant frequency shifts, films should be designed for maximum capacitive sensitivity (to induce change in antenna resonant frequency) as opposed to only resistance (bandwidth).

In the near future, EIS characterization will be employed to verify the proposed RC-parallel circuit model for bulk SWNT-PSS/PVA thin films. Methods such as complex non-linear least square fitting (LEVM) will be employed to fit strain sensor responses. Layer-by-layer nano-fabrication parameters will be explored to optimize capacitive strain sensitivity. Furthermore, numerical analyses will be conducted to correlate fabrication parameters with the inductive coil antenna strain sensing performance.

### Acknowledgements

This research is funded by the National Science Foundation (Grant Number CMS-0528867). The authors would like to express their gratitude to Professor Victor Li and the ACE-MRL group for offering the use of their MTS-810 load frame during the experimental phase of this study.

### References

- Andrews, R., D. Jacques, A.M. Rao, T. Rantell, F. Derbyshire, Y. Chen, J. Chen, and R.C. Haddon (1999), "Nanotube Composite Carbon Fibers," *Applied Physics Letters*, **75**(9), 1329–1331.
- Barsoukov, E. and J. Ross Macdonald ed. (2005), *Impedance Spectroscopy Theory, Experiment, and Applications*, John Wiley & Sons, Hoboken, New Jersey.
- Baughman, R.H., A.A. Zakhidov, and W.A. de Heer (2002), "Carbon Nanotubes – The Route Towards Applications," *Science*, **297**, 787–792.

- Dai, L., "Carbon Nanotube Sensors," *SPIE 9<sup>th</sup> Annual International Symposium on Smart Structures and Materials*, **4695**, San Diego, CA, 2002. Proceedings, 237–244.
- Decher, G. (1997), "Fuzzy Nanoassemblies Toward Layered Polymeric Multicomposites," *Science*, **277**, 1232–1237.
- Dharap, P., Z. Li, S. Nagarajaiah, and E.V. Barrera (2004), "Nanotube Film Based on Single-Wall Carbon Nanotubes for Strain Sensing," *Nanotechnology*, **15**, 379–382.
- Finkenzerler, K. (1999), *RFID Handbook: Radio-Frequency Identification Fundamentals and Applications*, John Wiley & Son, West Sussex, England.
- Iijima, S. (1991), "Helical Microtubules of Graphitic Carbon," *Nature*, **354**, 56–58.
- Kong, J., N.R. Franklin, C. Zhou, M.G. Chapline, S. Peng, K. Cho, and H. Dai (2000), "Nanotube Molecular Wires as Chemical Sensors," *Science*, **287**, 622–625.
- Kotov, N.A. (2001), "Ordered Layered Assemblies of Nanoparticles," *MRS Bulletin*, **26**, 992–997.
- Lee, Y. (1998), *RFID Coil Design*, Microchip Technology.
- Li, Z., P. Dharap, S. Nagarajaiah, E.V. Barrera, and J.D. Kim (2004), "Carbon Nanotube Film Sensors," *Advanced Materials*, **16**(7), 640–643.
- Loh, K.J., J.P. Lynch, and N.A. Kotov (2005), "Conformable Single-Walled Carbon Nanotube Thin Film Strain Sensors for Structural Monitoring," *The 5<sup>th</sup> International Workshop on Structural Health Monitoring*, Stanford, CA, September 12–15, 2005.
- Loh, K.J., J.P. Lynch, B.S. Shim, and N.A. Kotov (2006), "Identification of Nano-Fabrication Parameters for Optimization of Single-Walled Carbon Nanotube/Polyelectrolyte Thin Film Strain Sensors," *Smart Materials and Structures* (submitted May 2006).
- Lynch, J.P. and K.J. Loh (2005), "A Summary Review of Wireless Sensors and Sensor Networks for Structural Health Monitoring," *Shock and Vibration Digest*, **38**(2), 91–128.
- Mamedov, A.A., N.A. Kotov, M. Prato, M.D. Guldi, J.P. Wicksted, and A. Hirsch (2002), "Molecular Design of Strong Single-Wall Carbon Nanotube/Polyelectrolyte Multilayer Composites," *Nature Materials*, **1**, 190–194.
- Meyyappan, M. ed. (2005), *Carbon Nanotubes Science and Applications*, CRC, Boca Raton, FL.
- Minot, E.D., Y. Yaish, V. Szaonova, J-Y. Park, M. Brink, and P.L. McEuen (2003), "Tuning Carbon Nanotube Band Gaps with Strain," *Physical Review Letters*, **90**(15), 156401/1–156401/4.
- Mita, A. and S. Takahira (2004), "Damage Index Sensors for Smart Structures," *Structural Engineering and Mechanics*, **17**(3–4), 331–346.
- Olek, M., J. Ostrander, S. Jurga, H. Mohwald, N. Kotov, K. Kempa, and M. Giersig (2004), "Layer-by-Layer Assembled Composites from Multiwall Carbon Nanotubes with Different Morphologies," *Nano Letters*, **4**(10), 1889–1895.
- Ong, K.G., K. Zeng, and C.A. Grimes (2002), "A Wireless, Passive Carbon Nanotube-Based Gas Sensor," *IEEE Sensors Journal*, **2**(2), 82–88.
- Paloniemi, H., M. Lukkarinen, T. Aaritalo, S. Areva, J. Leiro, M. Heinonen, K. Haapakka, and J. Luddari (2006), "Layer-by-Layer Electrostatic Self-Assembly of Single-Wall Carbon Nanotube Polyelectrolytes," *Langmuir*, **22**, 74–83.
- Peng, S., J. O’Keeffe, C. Wei, K. Cho, J. Kong, R. Chen, N. Franklin, and H. Dai, "Carbon Nanotube Chemical and Mechanical Sensors," *The 3<sup>rd</sup> International Workshop on Structural Health Monitoring*, Stanford, CA, 2001. Proceedings, 1–8.
- Rouse, J.H. and P.T. Lillehei (2003), "Electrostatic Assembly of Polymer/Single Walled Carbon Nanotube Multilayer Films," *Nano Letters*, **3**(1), 59–62.
- Salvetat, J-P., J-M. Bonard, N.H. Thomson, A.J. Kulik, L. Forro, W. Benoit, and L. Zuppiroli (1999), "Mechanical Properties of Carbon Nanotubes," *Applied Physics A*, **69**, 255–260.
- Tombler, T.W., C. Zhou, L. Alexseyev, J. Kong, H. Dai, L. Liu, C.S. Jayanthi, M. Tang, and S-Y. Wu (2000), "Reversible Electromechanical Characteristics of Carbon Nanotubes Under Local Probe Manipulation," *Nature*, **405**, 769–772.
- Tsukagoshi, K., N. Yoneya, S. Uryu, Y. Aoyagi, A. Kanda, Y. Ootuka, and B.W. Alphenaar (2002), "Carbon Nanotube Devices for Nanoelectronics," *Physica B*, **323**, 107–114.
- Wood, J.R., Q. Zhao, M.D. Frogley, E.R. Meurs, A.D. Prins, T. Peijs, D.J. Dunstan, and H.D. Wagner (2000), "Carbon Nanotubes: From Molecular to Macroscopic Sensors," *Physical Review B*, **62**(11), 7571–7575.